

# Binders alternative to Portland cement and waste management for sustainable construction—part I

Journal of Applied Biomaterials &  
Functional Materials  
2018, Vol. 16(3) 186–202  
© The Author(s) 2018  
Reprints and permissions:  
sagepub.co.uk/journalsPermissions.nav  
DOI: 10.1177/2280800018782845  
journals.sagepub.com/home/jbf  


**Luigi Coppola<sup>1</sup>, Tiziano Bellezze<sup>2</sup>, Alberto Belli<sup>2</sup>, Maria Chiara Bignozzi<sup>3</sup>, Fabio Bolzoni<sup>4</sup>, Andrea Brenna<sup>4</sup>, Marina Cabrini<sup>1</sup>, Sebastiano Candamano<sup>5</sup>, Marta Cappai<sup>6</sup>, Domenico Caputo<sup>7</sup>, Maddalena Carsana<sup>4</sup>, Ludovica Casnedi<sup>6</sup>, Raffaele Cioffi<sup>8</sup>, Ombretta Cocco<sup>6</sup>, Denny Coffetti<sup>1</sup>, Francesco Colangelo<sup>8</sup>, Bartolomeo Coppola<sup>9</sup>, Valeria Corinaldesi<sup>2</sup>, Fortunato Crea<sup>5</sup>, Elena Crotti<sup>1</sup>, Valeria Daniele<sup>10</sup>, Sabino De Gisi<sup>11</sup>, Francesco Delogu<sup>6</sup>, Maria Vittoria Diamanti<sup>4</sup>, Luciano Di Maio<sup>9</sup>, Rosa Di Mundo<sup>11</sup>, Luca Di Palma<sup>12</sup>, Jacopo Donnini<sup>2</sup>, Ilenia Farina<sup>8</sup>, Claudio Ferone<sup>8</sup>, Patrizia Frontera<sup>13</sup>, Matteo Gastaldi<sup>4</sup>, Chiara Giosuè<sup>2</sup>, Loredana Incarnato<sup>9</sup>, Barbara Liguori<sup>7</sup>, Federica Lollini<sup>4</sup>, Sergio Lorenzi<sup>1</sup>, Stefania Manzi<sup>3</sup>, Ottavio Marino<sup>7</sup>, Milena Marroccoli<sup>14</sup>, Maria Cristina Mascolo<sup>15</sup>, Letterio Mavilia<sup>16</sup>, Alida Mazzoli<sup>2</sup>, Franco Medici<sup>12</sup>, Paola Meloni<sup>6</sup>, Glauco Merlonetti<sup>2</sup>, Alessandra Mobili<sup>2</sup>, Michele Notarnicola<sup>11</sup>, Marco Ormellese<sup>4</sup>, Tommaso Pastore<sup>1</sup>, Maria Pia Pedferri<sup>4</sup>, Andrea Petrella<sup>11</sup>, Giorgio Pia<sup>6</sup>, Elena Redaelli<sup>4</sup>, Giuseppina Roviello<sup>8</sup>, Paola Scarfato<sup>9</sup>, Giancarlo Scoccia<sup>10</sup>, Giuliana Taglieri<sup>10</sup>, Antonio Telesca<sup>14</sup>, Francesca Tittarelli<sup>2</sup>, Francesco Todaro<sup>11</sup>, Giorgio Vilardi<sup>12</sup> and Fan Yang<sup>4</sup>**

## Abstract

This review presents “a state of the art” report on sustainability in construction materials. The authors propose different solutions to make the concrete industry more environmentally friendly in order to reduce greenhouse gases emissions and consumption of non-renewable resources. Part I—the present paper—focuses on the use of binders alternative to

<sup>1</sup>Department of Engineering and Applied Sciences, University of Bergamo, Italy

<sup>2</sup>Department of Materials, Environmental Sciences and Urban Planning, Università Politecnica delle Marche, Ancona, Italy

<sup>3</sup>Department of Civil, Chemical, Environmental and Materials Engineering, University of Bologna, Italy

<sup>4</sup>Department of Chemistry, Chemical Engineering and Materials, Politecnico di Milano, Italy

<sup>5</sup>Department of Environmental and Chemical Engineering, University of Calabria, Italy

<sup>6</sup>Department of Mechanical, Chemical and Materials Engineering, University of Cagliari, Italy

<sup>7</sup>Department of Chemical, Materials and Production Engineering, University of Naples Federico II, Italy

<sup>8</sup>Department of Engineering, University of Naples Parthenope, Italy

<sup>9</sup>Department of Industrial Engineering, University of Salerno, Italy

<sup>10</sup>Department of Industrial and Information Engineering and Economics, University of L'Aquila, Italy

<sup>11</sup>Department of Civil, Environmental, Land, Building Engineering and Chemistry, Politecnico di Bari, Italy

<sup>12</sup>Department of Chemical Engineering, Materials and Environment, Sapienza University of Rome, Italy

<sup>13</sup>Department of Civil Engineering, Energy, Environment and Materials, Mediterranea University of Reggio Calabria, Italy

<sup>14</sup>School of Engineering, University of Basilicata, Italy

<sup>15</sup>Department of Civil and Mechanical Engineering, University of Cassino and Southern Lazio, Italy

<sup>16</sup>Department of Heritage, Architecture and Urban Planning, University of Reggio Calabria, Italy

## Corresponding author:

Luigi Coppola, Department of Engineering and Applied Sciences, University of Bergamo, Dalmine, Italy.

Email: luigi.coppola@unibg.it

Portland cement, including sulfoaluminate cements, alkali-activated materials, and geopolymers. Part 2 will be dedicated to traditional Portland-free binders and waste management and recycling in mortar and concrete production.

## Keywords

Building materials, concrete, Portland cement, sustainability, alternative binders, waste management

Date received: 21 December 2017; revised: 15 March 2018; accepted: 19 March 2018.

## Introduction

With the dawn of the 21st century, the world has entered an era of sustainable development. As a consequence, the concrete industry has to face two antithetical needs: how to feed the needs of the growing population, while being—at the same time—sustainable?

Sustainability in the construction industry can be achieved through three different routes (Figure 1), with reductions in consumption of gross energy, polluting emissions, and non-renewable natural resources. Different strategies can be identified along these three routes to make the concrete sector more environmentally friendly (Figure 2): (a) using alternative fuels and raw materials to reduce CO<sub>2</sub> emissions to produce Portland cement; (b) replacing Portland cement with low-carbon supplementary cementitious materials (SCMs); developing alternative low-carbon binders (alkali-activated materials, geopolymers, and calcium sulfoaluminate cements); and (c) reducing natural resource consumption through to waste management and recycling.<sup>1–3,4</sup>

Part 1 of this review—the present paper—deals with use of binders other than Portland cement. Part 2 will be dedicated to waste management and recycling in mortar and concrete production.

## Alternative binders to Portland cement

Different alternative binders to traditional Portland cement have been proposed, for example, sulfoaluminate cements, activated alkaline binders, and geopolymers.

### Sulfoaluminate cements

Calcium sulfoaluminate cements (CSA) have been applied since the end of the 1950s.<sup>5</sup> In the mid-1970s, CSA cement was produced on an industrial scale in China by burning limestone, bauxite, and gypsum at 1300–1350°C.<sup>6</sup> In China, CSA cements are treated as a special binder with rapid setting, shrinkage compensation, and high early-age strength. The main phase of CSA is tetracalcium trialuminate sulfate or ye'elimite (C<sub>4</sub>A<sub>3</sub>S̄). The amount of ye'elimite in CSA cement usually varies from 20% to 70%. Apart from ye'elimite, belite (C<sub>2</sub>S) is another main phase in CSA cement, while secondary phases may include C<sub>4</sub>AF, C<sub>3</sub>A, C<sub>12</sub>A<sub>7</sub>, and C<sub>6</sub>AF<sub>2</sub>.<sup>7</sup> CSA cement is a

sustainable cement when compared with ordinary Portland cement (OPC),<sup>8,9</sup> since less limestone is required due to the low CaO content in ye'elimite phase.<sup>8,10,11</sup> Moreover, more gypsum or anhydrite (CaSO<sub>4</sub>) is needed to prepare CSA cement; therefore, the CO<sub>2</sub> released in CSA cement production process is much less than that in OPC production.<sup>12</sup> Secondly, its calcination temperature is 100–150°C lower than that of OPC, which helps reduce coal consumption by 15% with respect to OPC.<sup>13</sup> Thirdly, CSA clinker is porous, which makes it easier to be ground,<sup>14</sup> and this further reduces energy consumption. However, the use of CSA cement to replace OPC 100% might encounter some adversities such as overly short setting time,<sup>13</sup> low pH,<sup>15</sup> high price,<sup>16</sup> and expansion risk.<sup>8</sup> Thereby, blending CSA with OPC might combine their advantages and improve properties such as expansion and setting time,<sup>17</sup> passivation ability of steel, and porosity.<sup>15</sup>

The hydration process of CSA cement has been studied.<sup>18–22</sup> The first hydration reaction in the presence of gypsum (C̄SH<sub>2</sub>) is:



The formation of ettringite (C<sub>6</sub>A<sub>3</sub>S̄H<sub>32</sub>), AFt, takes place mainly in the first hours.<sup>23</sup> When gypsum is depleted, ye'elimite forms monosulfate (C<sub>6</sub>A<sub>3</sub>S̄H<sub>12</sub>): AFm. Hydration of belite occurs at a later stage due to its low reactivity. Because the hydration products of ye'elimite contain amorphous AH<sub>3</sub>, reaction of belite in the presence of AH<sub>3</sub> will form stratlingite (C<sub>2</sub>ASH<sub>8</sub>) rather than C–S–H.<sup>24</sup> Most of the ye'elimite and gypsum react in the first 7 days, while most of the belite can be unhydrated even at 90 days.<sup>8</sup> In case of blended CSA/OPC cement, their hydration products depend highly on the ratio of OPC/CSA. For low OPC/CSA ratio, the hydration of OPC takes place later, several days after casting.<sup>25</sup> Alite (C<sub>3</sub>S) in OPC cement can react with AH<sub>3</sub>, which is the hydration product of ye'elimite at an early stage, to form stratlingite (C<sub>2</sub>ASH<sub>8</sub>) and portlandite (CH) at this early stage.<sup>17</sup> For high OPC/CSA ratio, alite can yield C–S–H and portlandite; the portlandite together with gypsum may then change the hydration reaction of ye'elimite to form 3C<sub>6</sub>A<sub>3</sub>S̄H<sub>32</sub>. The short setting time of CSA concrete is due to the quick and large formation of ettringite in the first hours.<sup>26</sup> Content of anhydrite in CSA

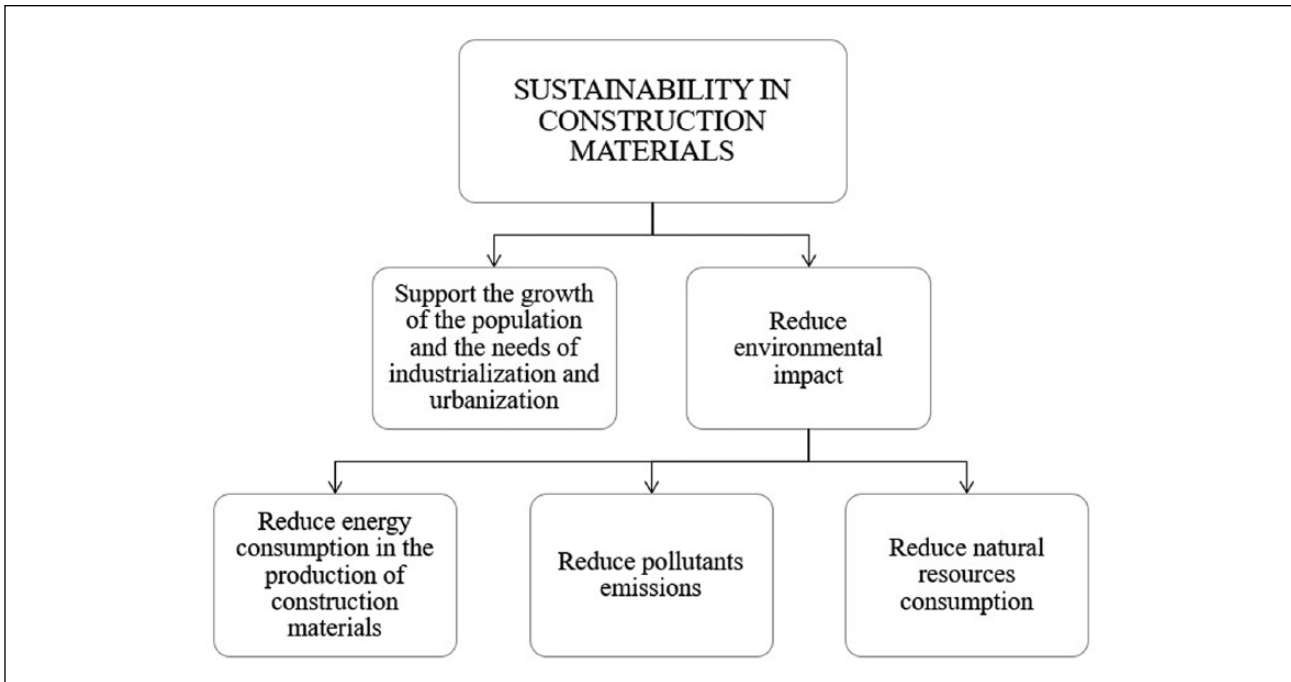


**Figure 1.** Main strategies to make the concrete sector more environmentally friendly.

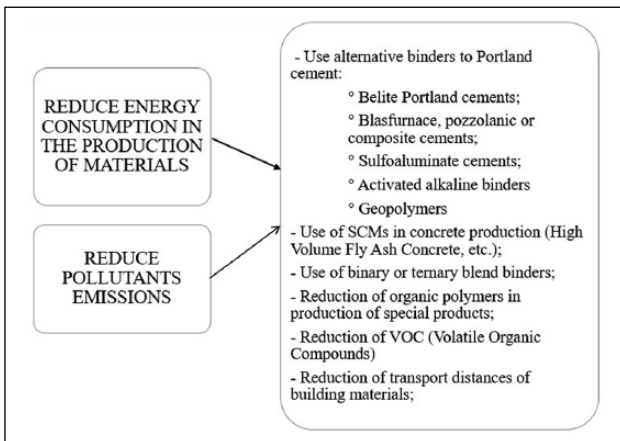


**Figure 2.** Reduction of energy and pollutants emission in construction materials production.

concrete can influence early-age compressive strength as well; increasing anhydrite content means more ye'elimite phase, which reacts at early stage and therefore forms more hydration products.<sup>27</sup>

Study performed on CSA cement paste have revealed that a bimodal pore distribution develops at a very early stage; lower porosity is dominant, but not connected with higher porosity.<sup>28</sup> Moreover, the average pore size of CSA concrete is smaller than that of OPC. The porosity of the CSA mortar decreases with the increase in anhydrite content and the decrease in w/c ratio.<sup>27</sup> A series of factors can influence the expansion of CSA concrete,<sup>8,29</sup> but ye'elimite

content plays an important role. If the proportion of ye'elimite is more than 50% in CSA cement, expansion, cracking, and loss of strength appear at later stage; the appropriate content of ye'elimite seems to range from 30% to 40%.<sup>30</sup>

Limited results are reported in the literature on the durability of concrete and mortars manufactured with CSA cement.<sup>27,31–33</sup> In particular, Quillis showed that CSA-based concretes exhibit excellent sulfate resistance but higher diffusion coefficient in Cl-rich environments with respect to OPC.<sup>13</sup> Moreover, despite conflicting results on the carbonation rate of mixtures containing CSA, it is evident that, similarly to OPC-concretes, carbonation depth is directly proportional to the water/binder ratio.<sup>31,34</sup>

### Alkali activated materials

Alkali-activated materials (AAMs), which were developed starting from the 1940s,<sup>35</sup> are obtained by reaction of an alkali metal source with amorphous or vitreous calcium-aluminosilicate precursors. The former is used to increase the pH of the reaction mixture thus accelerating the dissolution of the powders, while the composition of the latter determines the physical-chemical processes that produce hardening.<sup>36,37</sup> Microstructures, workability, and strength and durability of AAMs can be tuned by the proper combination of activators and precursors. Mix design of AAMs includes materials from both natural sources (metakaolin (MK) and pozzolans (P)) and by-products (slag (GGBS), fly ash (FA), and paper sludge

(PS)). AAMs can be classified according to the nature of the precursor (CaO–SiO<sub>2</sub>–Al<sub>2</sub>O<sub>3</sub> system) into two main categories: (a) high calcium and (b) low calcium. When aluminosilicate sources (MK, FA) are used, a (Na,K)<sub>2</sub>O–Al<sub>2</sub>O<sub>3</sub>–SiO<sub>2</sub>–H<sub>2</sub>O system is generated. This can be considered a subset of AAMs usually referred as geopolymers, characterized by a peculiar pseudo-zeolitic network structure.<sup>38–40</sup> When slag is used as precursor, a (Na,K)<sub>2</sub>O–CaO–Al<sub>2</sub>O<sub>3</sub>–SiO<sub>2</sub>–H<sub>2</sub>O system is produced. It is activated under moderate alkaline conditions,<sup>41,42</sup> and hardening is produced by the formation of a C–A–S–H gel. A combination of the preceding two systems is also possible,<sup>43,44</sup> where hardening is due to the formation of a C–A–S–H and (N,C)–A–S–H gels network.<sup>45</sup>

The reactive powder used to produce the calcium-rich binder is blast furnace slag originating from the purification process of iron ore to iron.<sup>46</sup> Ground granulated blast furnace slag (GGBFS) is a mixture highly glassy phases with a composition close to that of gehlenite and akermanite: (31–38%) SiO<sub>2</sub>, (38–44%) CaO, (9–13%) Al<sub>2</sub>O<sub>3</sub> and (7–12%) MgO, and S, Fe<sub>2</sub>O<sub>3</sub>, MnO, and K<sub>2</sub>O with percentages of less than 1%. When it is used to produce AAMs, parameters affecting GGBFS reactivity are the vitreous phase content (85–95%wt), its degree of depolymerization (DP, from 1.3 to 1.5), and its specific surface (400–600 m<sup>2</sup>/kg).<sup>36</sup>

Slag alkaline activation consists of dissolution of the glassy particles,<sup>35–37</sup> nucleation and growth of the initial solid phases, interactions and mechanical binding at the boundaries of the phases formed, ongoing reaction via dynamic chemical equilibria, and diffusion of reactive species through reaction products formed at advanced times of curing.<sup>47,48</sup> At the early stages, the alkaline solution reacts with dissolved species generating the outer C–A–S–H. At later stages, the inner C–A–S–H gel is produced by ongoing reactions of the undissolved portions of the slag particles through a diffusion mechanism.<sup>49</sup>

The cations and anions of the activator play a specific role in the activation process. When hydroxides are used, the OH<sup>−</sup> acts as a catalyst and is responsible for the pH increase, thus allowing precursor dissolution and the formation of stable hydrates.<sup>50</sup> Slag-based binder can be prepared using 2–4 M solution with Na<sub>2</sub>O content less than 5% slag weight to guarantee mechanical properties and reduce efflorescence.<sup>51–54</sup> When sodium silicate is used, the gel is characterized by lower Ca/Si and a less ordered structure. In both the cases, the gel is comprised of coexisting 11 and 14 Å disordered tobermorite-like phases,<sup>48</sup> with a Ca/Si ratio (0.9–1.2) lower than in hydrated Portland cement system. AFm type phases or strätlingite are formed when NaOH or silicate, respectively, are used.<sup>55,56</sup> If raw materials contain high amounts of MgO,<sup>57,58</sup> hydrotalcite (Mg<sub>6</sub>Al<sub>2</sub>(OH)<sub>16</sub>·4H<sub>2</sub>O) is produced, while in the presence of low MgO (<5%) and high Al<sub>2</sub>O<sub>3</sub> contents, zeolites are often found in the reaction products.<sup>59</sup>

### MK- and FA-based geopolymers

As a general statement, MK can be said to be the “model system” for studying the activation process of AAMs.<sup>60–68</sup> MK (Al<sub>2</sub>O<sub>3</sub>:2SiO<sub>2</sub>) is a natural pozzolanic material obtained by the calcination of kaolin at 500–900°C.<sup>69,70</sup> MK consists of plate-like particles with a specific surface area generally between 9 and 20 m<sup>2</sup>/g.<sup>71</sup> MK pastes usually require a liquid/MK > 0.6 by mass,<sup>72</sup> and MK mortars need ~1.0.<sup>73,74</sup> In general, MK geopolymers set within 24 h. Conversely, MK geopolymers have a higher reaction rate and a faster strength gain with respect to FA geopolymers,<sup>75,76</sup> because of the presence of secondary minerals in the kaolinite clay,<sup>77,78</sup> the fineness of the particles,<sup>79</sup> and the reaction temperature.<sup>80,81</sup> Hydrothermal ageing (95°C) because of major formation of crystalline zeolite, is responsible for strength loss.<sup>76</sup> Moreover, the thermal treatment of MK mixtures at 80°C accelerates strength development, but the final strength is lower than that of specimens cured at ambient temperature.<sup>73</sup> In geopolymers, SiO<sub>2</sub>/Al<sub>2</sub>O<sub>3</sub>, Na<sub>2</sub>O/Al<sub>2</sub>O<sub>3</sub> and Na<sub>2</sub>O/H<sub>2</sub>O influence mechanical properties. Compressive strength and Young's modulus were found to be dependent on alkali type (Na or K) and Si/Al ratio.<sup>82</sup> However, at the same compressive strength, the authors found that the modulus of elasticity is lower in geopolymers than in OPC mortars due to the large number of small pores that promote the formation of micro-cracks.<sup>75,83</sup> K-based geopolymers produce a higher compressive strength than Na-based ones, and the increase of SiO<sub>2</sub>/Al<sub>2</sub>O<sub>3</sub> also increases mechanical strength.<sup>84</sup> Davidovits indicated that the optimum Na<sub>2</sub>O/Al<sub>2</sub>O<sub>3</sub> and SiO<sub>2</sub>/Al<sub>2</sub>O<sub>3</sub> ratios are 1 and 4, respectively,<sup>85</sup> while most researchers reported an optimum SiO<sub>2</sub>/Al<sub>2</sub>O<sub>3</sub> of 3–3.8,<sup>54,86</sup> The increase in Si/Al ≥ 3 leads to chemical instability in air, with efflorescence formation on the surface attributed to the high residual free alkali cations.<sup>87</sup> Usually, increasing Na<sub>2</sub>O/H<sub>2</sub>O leads to improved dissolution ability and mechanical strength development of clay-based geopolymers.<sup>74,84,88,89</sup> Geopolymers prepared only with MK are highly susceptible to shrinkage both at room and elevated temperatures,<sup>72,90–94</sup> because of their high water requirement.

Concerning the effect of aggressive/pollutant substances on MK concretes durability,<sup>95–98</sup> Palomo et al. found that MK geopolymers were stable if immersed in seawater, Na<sub>2</sub>SO<sub>4</sub> solution (4.4%), and H<sub>2</sub>SO<sub>4</sub> solution (0.001 M) for up to 90 days.<sup>99</sup> On the contrary, Mobili et al. noticed crack formation on MK geopolymers exposed to Na<sub>2</sub>SO<sub>4</sub> solution (14%), not present in FA geopolymers with the same activators.<sup>75</sup> Gao et al. found that MK geopolymers remain sound after 28 days in HCl solution (pH 2).<sup>100–102</sup> The capillary water absorption of MK-based geopolymers is higher than blended blast furnace slag,<sup>103,104</sup> FA, or OPC geopolymers.<sup>75</sup> Currently, researchers are studying MK-based geopolymers also to produce non-structural plasters with lightweight

aggregates for thermal insulation,<sup>105–110</sup> and to be used as mortars able to adsorb volatile organic compounds (VOCs).<sup>111–115</sup>

Another trend is to produce geopolymers suitable for refractory applications, adding a foaming agent, H<sub>2</sub>O<sub>2</sub>, or Al powder.<sup>106,116,117</sup> Results show that only Al-geopolymers are successfully converted to crack-free ceramics upon heating.<sup>116</sup> The partial substitution of MK with FA also has a positive influence on both thermal resistance and compressive strength,<sup>106,118</sup> thanks to the lower water demand and thus the lower free water evaporation. Foams have much lower thermal conductivity (0.15–0.4 W/m·K) than the solid geopolymer (0.6 W/m·K).<sup>119</sup> The thermal conductivity increases with increased Si/Al ratio, because of the increased connectivity, reduced porosity, and finer pore size distribution.<sup>120,121</sup> Moreover, increasing the K/Al ratio also increases the foaming efficiency (final volume/initial volume).<sup>122</sup> Geopolymers derived from a K-based activator dissolve or degrade more readily compared with Na-based geopolymers whether foamed or not.<sup>123,124–126</sup>

Researchers have investigated “one-part” MK geopolymers, obtained by adding only water to the dry materials, avoiding the use of caustic solutions, by the calcination of the clay material with a powdered activator, such as NaOH or KOH,<sup>127</sup> soluble sodium silicate,<sup>128</sup> sodium carbonate,<sup>129</sup> or by using an alkali-rich by-product, such as potassium-rich biomass ash.<sup>130</sup>

FA is an industrial byproduct derived from coal-fired power stations with a highly variable composition, dependent on the coal source and burning conditions.<sup>131</sup> Particle size distribution, chemical composition and crystalline/glassy phases of the precursor are key factors that need to be understood, since they control the precursor reactivity and solubility in alkaline solutions.<sup>132</sup> It was found that the geopolymer microstructure is highly influenced by particle fineness, amorphous phase composition, and oxide content (particularly Fe<sub>2</sub>O<sub>3</sub> and CaO).<sup>133,134</sup> The lower Na<sub>2</sub>O/SiO<sub>2</sub> molar ratio, the higher the performances in terms of water absorption and mechanical properties.<sup>135</sup> Geopolymers showed good thermal stability after firing due to the formation of new crystalline phases.<sup>136</sup> Developing a comprehensive knowledge of precursors is a fundamental and critical step in commercializing geopolymer products. For example, a preliminary study demonstrated the use of geopolymer mortars for strengthening of concrete structures.<sup>137</sup> As workability is one of the main requirements, research on superplasticizers suitable for fly ash geopolymers needs to be emphasized.<sup>138–145,146</sup>

### Clayey sediments and sludge for geopolymers

Geopolymers are attractive because natural and industrial silico-aluminates wastes may be used as precursors. The exploration for alternative low cost and easily available materials led among others to “normal clays”. Clayey

sediments consist of different clay minerals; these are widely available all over the world, and offer significant reactivity after a thermal activation process.<sup>147</sup> Among silico-alumina wastes, reservoir sediments are worthy of consideration. Sediments should be removed periodically to avoid reduction in reservoir capacity. There are more than 7000 large reservoirs in the European Union (EU), of which 564 are in Italy. These data show that regular dredging operations can produce huge amounts of sediment. In this regard, some possibilities have been explored as raw materials in production of artificial aggregates, bricks and cement.<sup>148–153</sup> Studies aimed at extending these possibilities in the field of geopolymer materials have been reported by several authors.<sup>154–156</sup>

SiO<sub>2</sub> and Al<sub>2</sub>O<sub>3</sub> are the main components in sediments, while CaO and Fe<sub>2</sub>O<sub>3</sub> are present in lower concentrations; K<sub>2</sub>O, MgO, and Na<sub>2</sub>O are present in minimum percentages. The main mineralogical phases detected by X-ray diffraction analysis are quartz, calcite, clay phases, and feldspars. A pre-treatment of the sediment is always necessary in order to enhance the reactivity in alkaline environments. Messina et al. showed that 750°C is the optimal pre-treatment temperature for the production of concrete blocks and geopolymer mortars.<sup>157</sup> Indeed, the <sup>27</sup>Al NMR peak at 0 ppm related to octahedral Al (Figure 3) and absorbance FT-IR peaks at 3697, 3620, and 3415 cm<sup>-1</sup> were absent or greatly dampened, evidencing the collapse of the ordered clay structure.

The prevailing chemical components of the sediments are silica and alumina, thus making sediments good geopolymer precursors. However, within the wide range of natural and artificial silico-aluminates, the SiO<sub>2</sub>/Al<sub>2</sub>O<sub>3</sub> ratio in this case is quite high, such to make the alkali aluminate activation and/or the addition of alumina-rich additives an interesting alternative. Aluminate activation was studied in the manufacture of precast building blocks, with encouraging results.<sup>158</sup> Regarding alumina-rich additives, water potabilization sludge is another key residue produced by reservoir management activities. These wastes are based on flocculation-clarification processes using alumina coagulants.<sup>159</sup> The amount of sludge generated, and its chemical composition, depend mainly on the chemical and physical characteristics of the water, the efficiency of the removal process, and the type and dose of coagulant. The amount of sludge can be roughly estimated in the range of 1–5% of the total amount of untreated water.<sup>159</sup> This waste has been studied in only a few studies, mainly with regard to potential reuse in the construction industry.<sup>157,160–166</sup>

Management of the huge amounts of sediments coming from dredged activities is an important issue to be solved in many countries worldwide. Clean dredged materials can be used for construction fill, brick or asphalt manufacturing, topsoil and marine projects. Recently, Lirer et al. proposed dredged sediments with FAs in the production of

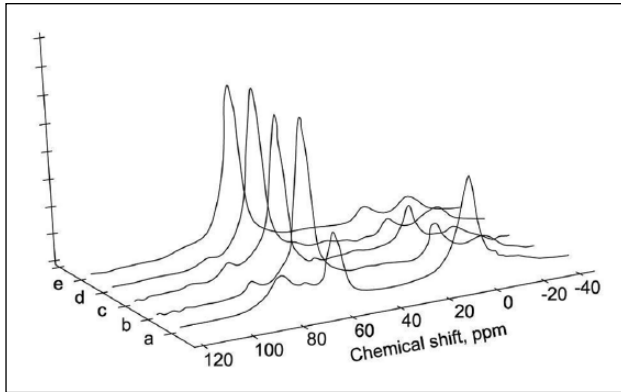


**Figure 3.**  $^{27}\text{Al}$  NMR resonance spectra of Occhito sediment before thermal treatment (a), after thermal treatment at  $650^\circ\text{C}$  for 1 h (b), at  $650^\circ\text{C}$  for 2 h (c), at  $750^\circ\text{C}$  for 1 h (d), at  $750^\circ\text{C}$  for 2 h (e).

geopolymers.<sup>165</sup> Regarding the environmental impact, the values of hazardous elements classify geopolymers as non-dangerous materials. Therefore, these preliminary results suggest that this methodology could represent a starting point for the investigation of possible beneficial uses of polluted sediments in geopolymeric matrices.

### Corrosion behavior in alternative binders-based matrix

Replacement of Portland cement with alternative binders, especially CSA cements and AAMs, open the theme of protection of reinforcements in these new concretes.<sup>168–170</sup> Data seem to indicate that the durability of CSA concretes is at least comparable to that of traditional Portland cement mixtures, but they also evidence the need to perform long-term tests in order to recognize the corrosion protection mechanism.<sup>24</sup> The protective capacity of the CSA-matrix has been confirmed by positive experiences of these structures in China, in which no rebar corrosion occurred after 14 years of exposure.<sup>171</sup> However, little information is given about the actual aggressive environmental conditions. Most works available are devoted to the study of hydration products in the very early period but only a few papers have addressed the corrosion behavior of reinforcements by means of electrochemical techniques. Potential measurements performed in a few experimental works evidence difficulties in achieving proper values of passive rebars due to the low alkali content of the pore water.<sup>172</sup> Studies on the durability of mixtures manufactured with such binders address only a few aspects—carbonation and chlorides—neglecting relevant aspects governing the corrosion process.<sup>13,28,173,174</sup>

The main hydration product of CSA cement is ettringite, which does not provide  $\text{OH}^-$ . The pH values of two pure CSA concretes with 0.5 w/c were 10.23 and 10.53, respectively, after 90 days.<sup>15</sup> In another case, w/c 0.45

CSA mortar showed low pH values (around 6) of the pore solution at 7 days after casting.<sup>172</sup> However, a high pH, around 13, within first 60 days has been observed by using a CSA cement paste with w/c 0.8.<sup>175</sup> An exhaustive investigation on two CSA cement pastes with w/c 0.72 and 0.8 revealed that, in the case of w/c 0.72 CSA cement paste, within the first hours, the pH was as low as 10.3–10.7 due to the fact that the initial saturated pore solution was dominated by aluminate, calcium, and sulfate; after 16 h, calcium and sulfate concentrations decreased noticeably due to the depletion of gypsum, thus the pH was around 11.8; after 28 days, the pH value reached 12.7 due to the ongoing release of alkali ions of CSA clinker and the increase of alkali concentrations caused by the consumption of the pore fluid by the formation of hydrates; while w/c 0.8 CSA cement paste showed a similar trend, but a slight higher pH at each stage.<sup>19</sup>

Ettringite is susceptible to carbonation.<sup>13,14</sup> It seems that the carbonation resistance of CSA concrete is weaker (Figure 4) than that of OPC concrete.<sup>176</sup> However, an investigation on two CSA concrete samples suggested that the carbonation resistance of CSA concrete is comparable with that of OPC concrete; high-strength CSA concrete has excellent carbonation resistance.<sup>32</sup> It was found that the carbonation resistance of CSA mortar increased along with the anhydrite content, as well as the decrease of w/c; meanwhile it was also found that carbonation changed the strength performance of CSA mortar due to the modification of porosity caused by carbonation.<sup>27</sup>

Lower chloride penetration resistance of CSA concrete was observed when compared with OPC concrete.<sup>13</sup> Conversely, low chloride diffusion coefficients of CSA concretes with different strengths were obtained when compared with their OPC counterparts.<sup>177</sup> To enhance the chloride penetration resistance of CSA concrete, modifying AFm/AFt through varying the gypsum content with the hope to let more AFm bind chlorides, was carried out.<sup>178</sup> Besides, good sulfate resistance of CSA concrete has been reported.<sup>13–15</sup> In the case of blended CSA cement, it was shown that increasing OPC in blended CSA cement (15%–85%) can improve the pH.<sup>179</sup>

Currently, there are very few publications dealing with the passivation of steel embedded in CSA concrete. Steel in CSA mortar showed a higher corrosion rate than steel in OPC mortar exposed to 3.5% NaCl solution.<sup>172</sup> Half-cell potential measurement showed that steel embedded in the CSA mortar was depassivated, showing a high corrosion rate in 3.5% NaCl solution, due to the low pH (around 6) of the pore solution of CSA mortar. However, the corrosion potential and corrosion rate of steel embedded in w/c ratio 0.55 CSA concrete with a pH value of 11.5 showed the passivation of embedded steel, even in concrete exposed to an environment at 95% relative humidity and  $40^\circ\text{C}$ , or immersed in water.<sup>176</sup> Mortar made with 100% CSA cement (pH 11.88) was not capable of passivating

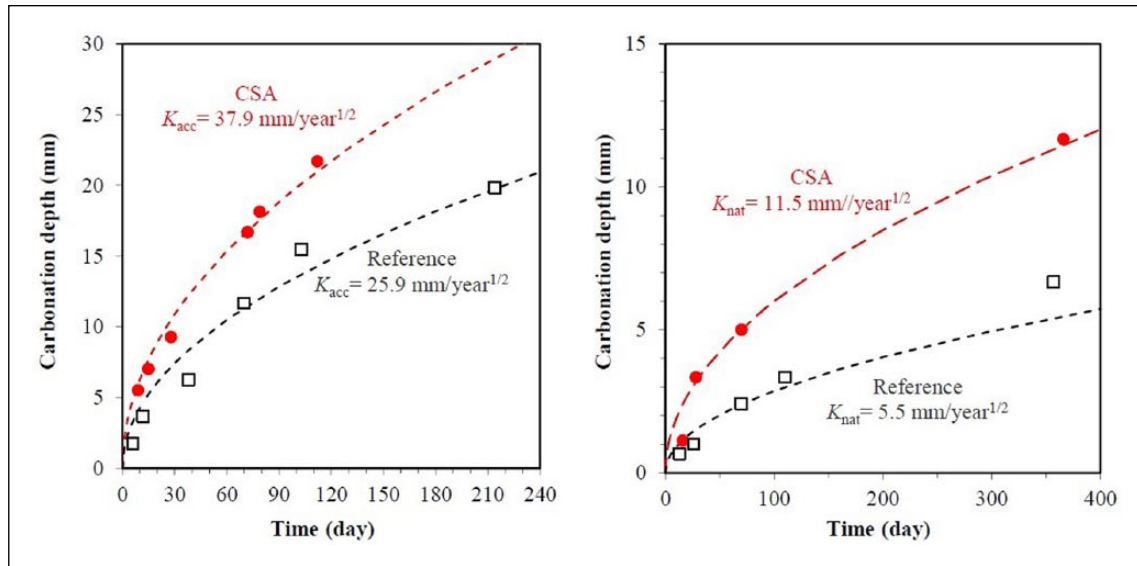


**Figure 4.** Time evolution of carbonation depth of CSA and reference OPC concrete under accelerated test (on the left) and indoor exposure (on the right). CSA: calcium sulfoaluminate cements; OPC: ordinary Portland cement.

steel; however, CSA cement blended with 15% OPC (pH 11.32) was enough to guarantee the passivation of steel.<sup>15</sup>

The pH of alkali activated binders is very high at initial stages due to the presence of activators, leading to the common conclusion that no corrosion issues can occur. However, the pH tends to decrease under endogenous conditions to values well below the limits for steel passivation in absence of chlorides because these types of binders consume alkalinity during the hydration process.<sup>180</sup> In addition, very scattered pH values are reported, and several doubts have still to be solved in terms of corrosion behavior of reinforcement due to the very different mineralogical composition of precursors.<sup>181</sup> In addition, the role of alkalinity reservoir should be well taken into account for CSA and AAMs binders, which are generally prone to consume calcium hydroxide rather than produce it, as does Portland cement.<sup>13</sup> The protectiveness is attributable not only to the pH, but also to the ability of OPC concrete to bind its own chlorides, leading to a lower amount of free chlorides. The main factors influencing the critical chlorides content for pitting initiation are alkalinity and the concrete-reinforcement interface characteristics.<sup>182–185</sup> The effect of alkalinity on localized corrosion initiation can be described in terms of chlorides-hydroxyl ions critical molar ratio, usually assumed equal to 0.6.<sup>168,184–193</sup> The critical chloride threshold in OPC concretes is much higher due to oversaturation of calcium hydroxide.<sup>194</sup> This leads to an increase in critical molar ratio at values exceeding 2.<sup>183,195</sup> This difference can be ascribed to the buffer ability by calcium hydroxide. The presence of this phase directly in contact with the carbon steel surface

represents a reservoir of alkalinity, which contrasts the pH drop due to localized corrosion initiation.

On the contrary, much attention should be paid to innovative binders due to the great compositional variability of the raw materials, usually industrial by-products. Chloride contamination can be non-negligible, leading to an increased risk of localized corrosion, especially in the first period when alkalinity has not yet reached a sufficient level to maintain stable passivity.

Mobili studied also the corrosion behavior of carbon and galvanized bars embedded in pure FA and MK geopolymers with the same strength class compared to OPC mortars.<sup>75,196,197</sup> During the curing period, geopolymers prolong the active state of rebars, but, after 10 days, corrosion rates ( $v_{\text{corr}}$ ) decreased to moderate values (around  $10 \mu\text{m}/\text{year}$ ) in all mortars.<sup>75</sup> During wet/dry (w/d) cycles in 3.5% NaCl solution,<sup>198</sup> MK geopolymers showed the greatest corrosion of embedded rebars and the highest consumption of the galvanized coating because of the higher porosity compared to FA and OPC geopolymers.<sup>199,200</sup> Aguirre-Guerrero studied the chloride-induced corrosion in OPC concrete coated with an alkali-activated mortar (90% MK (or FA) and 10% OPC); the MK geopolymer coating exhibited the best performances.<sup>201</sup>

Accelerated carbonation ( $\text{CO}_2 = 3 \text{ vol.}\%$ ) on slag/MK geopolymers shows that carbonation occurs faster as MK content increases and leads to a reduction in compressive strength.<sup>202</sup> Moreover, accelerated carbonation at 50%  $\text{CO}_2$  on MK-based geopolymers forms large amounts of sodium bicarbonate, leading to a lower pH of the pore solution; while the formation of sodium carbonate in natural conditions does not lead to a pH below 10.5 after 1 year.<sup>203</sup>

### Reinforcement less sensitive to corrosion

Carbonation or chloride-induced corrosion are the main issues in reinforced concrete structure manufactured with different types of binders. In carbonated concrete without chlorides, stainless steel rebars are passive.<sup>204,205</sup> For galvanized steel, the presence of an external layer of pure zinc and its thickness is of primary importance to form a passive film; in contact with alkaline solutions, if the pH does not exceed 13.3, a layer of calcium hydroxyzincate is formed and zinc is passivated.<sup>206</sup>

In chloride-contaminated concrete, the onset of corrosion occurs if a chloride threshold is exceeded. Even though the measurement of this threshold is not easy, some major factors have been identified: the pH, the potential of the steel and voids at the steel/concrete interface; for carbon steel in aerated concrete at 20°C, critical chloride threshold is generally in the range 0.4–1% by cement mass.<sup>206</sup> In the case of stainless steels, chemical composition is also important: corrosion resistance is improved by increasing Cr and Mo content, while probably the role of Ni is beneficial in alkaline environments and Mn appears to have worsening effect: for example, critical chloride threshold at 20°C in aerated alkaline concrete for typical 18%Cr and 8% Ni AISI 304L steel (1.4307 according to EN) is a minimum 5% of cement mass for pickled surface, and lowers in the presence of a welding scale.<sup>206–211</sup> Galvanized steels has a good resistance to chloride-induced corrosion, even if not comparable to stainless steels: in aerated concrete the critical chloride content is maximally 1–1.5%.<sup>206</sup>

Few papers have been published about the performance of stainless or galvanized steels in new binders matrix.<sup>75,139,199,212,213</sup> Moreover, results are not always consistent. Most researchers agree that the chloride concentration in alkali activated slag mortars is lower than in traditional mortars.<sup>139,199</sup> This effect has been attributed to the lower porosity and the different chloride binding capacity: while in Portland cement mortars chlorides form low solubility calcium-containing compounds, in geopolymers, since calcium content is very low, the chloride binding effect is negligible.

The pH of the pore solution is a matter of discussion. Some authors stated, without indicating any practical measurement, that pH is highly alkaline,<sup>212</sup> or more alkaline than traditional mortars.<sup>75</sup> On the contrary, other authors report pH values, measured by the leaching method, for alkali-activated mortars similar to that of CEM II A-L 42.5 R-based mortars (between 12.8 and 13.2), but after exposure to 11 cycles of wetting with chloride solution and drying, the pH of alkali-activated mortars was found to be 10.5–10.7 against 12.2 for cement-based mortars.<sup>139</sup>

Corrosion of low nickel (4.3%) manganese (7.2%) austenitic stainless steel with 16.5% Cr is compared with traditional stainless steel AISI 304 (1.4301 according to EN

10088-1) in alkali-activated FA mortars characterized by high alkalinity (the authors reported pH higher than 13, although few details are provided).<sup>212</sup> Both stainless steels exhibited passive behavior up to 2% chloride content, while carbon steel suffered corrosion in 0.4% chlorides. In another report, stainless steels (traditional type AISI 304 and low nickel) in carbonated mortars subjected to accelerated chloride exposure suffered localized corrosion.<sup>213</sup> Analysis of rebars after a 2-year exposure showed that in alkali activated slag mortars the behavior was better than in OPC mortars. The authors attributed the improvement to the higher concentration of inhibiting bicarbonate/carbonate ions present in these binders.<sup>213</sup> The results are promising but not conclusive: on the one hand, chloride content 2% in alkaline mortar is not high enough to evaluate the long-term performance of stainless steel rebars,<sup>212</sup> since the chloride content is well below than the critical chloride threshold in alkaline concrete. On the other hand, the results of the other group show a little improvement of corrosion behavior in alkali-activated mortars vs traditional ones.<sup>213</sup> Concerning galvanized rebars, it has been mentioned that geopolymeric mortars can have two opposite effects: a delay in the passivation due to the higher pH (potentially negative), and a reduction in corrosion rate after some cycles of wetting with 3.5% NaCl.<sup>75,199</sup> Nevertheless, corrosion rate in alkali-activated slag mortars was found to be 50 µm/year. This value would lead to the consumption of the zinc layer (typically 150 µm) within a few years, so these results do not guarantee long-term performance of the galvanized rebar in geopolymeric mortars.

### Alkali-activated materials in repair and conservation

The issue of retrofitting and seismic upgrade of existing masonry buildings and reinforced concrete structures has become of primary interest due to the huge architectural heritage all over the world. This topic is extremely complex, especially because of many compatibility issues between existing structures and Portland cement repair mortars.<sup>214–217,218</sup> In fact, use of Portland cement mixtures on masonry structures can cause damage due to the presence of sodium and potassium ions, which can promote an alkali-aggregate reaction,<sup>219</sup> or, in the presence of wet environments and sulfur-rich natural stones,<sup>220</sup> it could determine the development of thaumasite and secondary ettringite, with expansion and cracking phenomena. Another key parameter for repair mortars is the elastic compatibility<sup>221,222</sup>: if Young's modulus of repair material is different from the substrate, it may create detachments and cracks. Finally, it is not possible to overlook the aesthetic compatibility between the original areas and those involved in maintenance works.<sup>223</sup>

Currently, natural hydraulic lime (NHL) represents the only binder that can be used in these contexts due to their



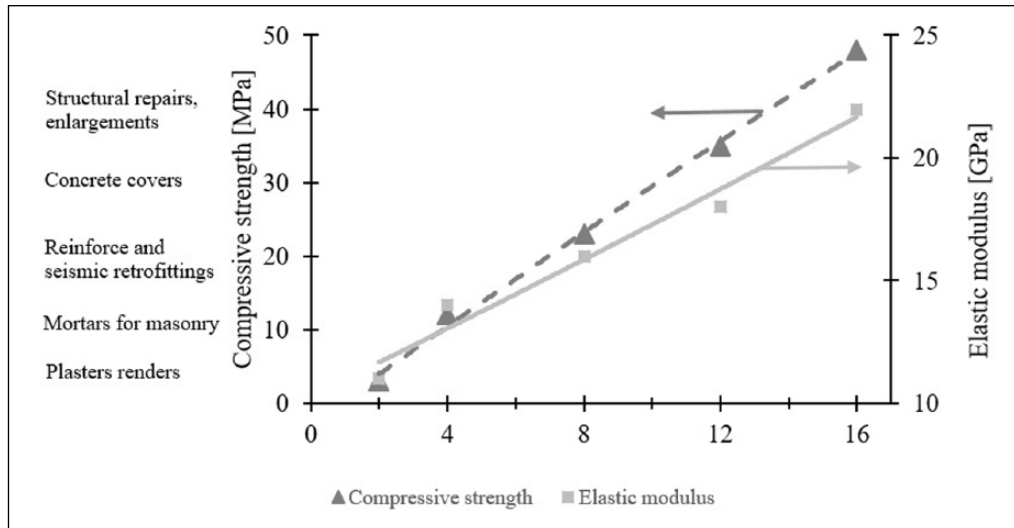


**Figure 5.** Compressive strength and elastic modulus of GGBFS-based mortars manufactured with blend of sodium metasilicate, potassium hydroxide, and sodium carbonate (7:3:1) at different activator/precursor ratios. GGBFS: Ground granulated blast furnace slag.

high compatibility with the substrates.<sup>224–226</sup> However, due to their low mechanical strength, NHL-based mortars often do not meet elasto-mechanical requirements, and, for this reason, are very often mixed with Portland cement.

The use of cement-free alkali-activated materials (AAM), such as GGBFS, could also be a suitable alternative to Portland cement mixtures.<sup>227–230</sup>

The key parameter that regulates most of properties of alkali-activated compounds is the precursor/activator ratio.<sup>231–236</sup>

A key aspect for use in maintenance is the possibility to tailor the strength and stiffness with the activator/precursor<sup>237–239</sup>; in particular, both the compressive strength and elastic modulus increased due to the high alkali-activator dosage in the mixture. Specifically (Figure 5), weakly alkali-activated GGBFS-based mortars can be used for plasters or masonry mortars while, in presence of high activator/precursor ratios, can be employed for seismic retrofitting or for reinforced concrete structures restoration.

Another key parameter of alkali-activated mortars is elastic modulus (Figure 5); several authors showed less rigidity of GGBFS-based matrix respect to reference mixtures with OPC,<sup>36,55,240,241</sup> at equal strength class due to the high shrinkage of AAM mortars that promote the formation of microcracks.<sup>83</sup> In particular, low activator/precursor ratios determine Young's modulus ranging from 10 to 15 GPa, while higher alkaline powders dosages cause an increase in GGBFS-based matrix-stiffness, and, consequently, elastic modulus increases up to 20 GPa. In the presence of substrates restraining the dimensional contraction of repair mortar, this property determines the development of low internal tensile stresses, and thus, a lower cracking risk.

In general, alkali-activated mortars and concretes show very high free shrinkage compared to conglomerates manufactured with traditional binders.<sup>242</sup> These problems are caused by the large amount of water not involved in the hydration reaction, which, by evaporating, creates dimensional contraction and markedly porosity of matrix. Furthermore, alkali-activated slag pastes have a much higher range of pore sizes within mesopore region than OPC pastes. The radius of pores where the meniscus forms seems to be a key parameter for shrinkage.<sup>243–245</sup>

Researchers note that, by increasing the water/binder, there is a growth in shrinkage due to two factors: the large amount of water able to evaporate, and the increase in binder paste/aggregates.<sup>246</sup> In addition, it is possible to note that shrinkage is also influenced by type and contents of alkaline activators.<sup>247</sup> Reduction of shrinkage can be achieved by optimizing the mix with ethylene glycol SRA or calcium oxide expansive agents. In addition, methyl cellulose and starch ether (M.S.) can also be added in order to reduce water evaporation at the fresh state.<sup>41,248,249</sup> In particular, the addition of blends based on ethylene glycol and calcium oxide can reduce free shrinkage by about 40% compared to reference GGBFS-mortars without admixtures (Figure 6).

Another issue with AAMs is the efflorescence caused by excess of sodium oxide remaining unreacted in the material due to a disequilibrium in the mix towards the sodium-based activators. The parameter that influences the quantity of efflorescence is the Na/Al molar ratio; conglomerates with higher Na/Al molar ratios show a higher extent of alkali leaching, indicating a stronger tendency towards efflorescence.<sup>250,251</sup>

In conclusion, from analysis of the strengths and weaknesses of AAMs, it turns out that alkali-activated mortars

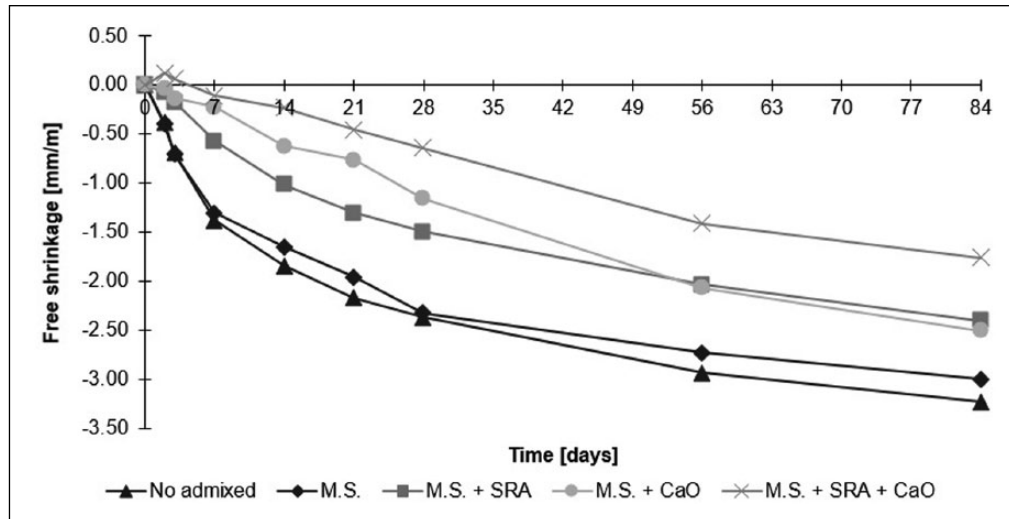


**Figure 6.** Free shrinkage of GGBFS-based mortars manufactured with blend of sodium metasilicate, potassium hydroxide, and sodium carbonate (7:3:1) at activator/precursor ratio equal to 0.12 with different type of admixtures. M.S.: methyl cellulose and starch ether; SRA: glycole ethylene-based SRA; CaO: calcium oxide-based expansive agent.

and concretes can be a reasonable alternative to traditional Portland cement-based mixtures or NHL-based conglomerates for restoration of ancient buildings.

#### Declaration of Conflicting Interests

The author(s) declared no potential conflicts of interest with respect to the research, authorship, and/or publication of this article.

#### Funding

The author(s) received no financial support for the research, authorship, and/or publication of this article.

#### References

- Coppola L, Coffetti D and Lorenzi S. Per uno sviluppo sostenibile delle costruzioni. Dalla cultura del "non più di" a quella del "non meno di". [For a sustainable development in construction industry: moving from the culture of "Not more than" to that of "Not less than."] *Structural* 2015; 28: 1–11.
- Gartner E and Hirao H. A review of alternative approaches to the reduction of CO<sub>2</sub> emissions associated with the manufacture of the binder phase in concrete. *Cem Concr Res* 2015; 78: 126–142.
- Coppola L, Coffetti D and Crotti E. Plain and ultrafine fly ashes mortars for environmentally friendly construction materials. *Sustainability* 10(3): 874.
- Coppola L, Belz G, Dinelli G, et al. Prefabricated building elements based on FGD gypsum and ashes from coal-fired electric generating plants. *Materials and Structures/Materiaux et Constructions* 1996; 29(189): 305–311.
- Budnikov P and Kravchenko I. Expansive cements. In: *Proceedings of the 5th International Congress on the Chemistry of Cement*. Tokyo, Japan. 1968; 4: 319–329.
- Zhang L, Su M and Wang Y. Development of the use of sulfo- and ferroaluminate cements in China. *Adv Cem Res* 1999; 11: 15–21.
- Tang SW, Zhu HG, Li ZJ, et al. Hydration stage identification and phase transformation of calcium sulfoaluminate cement at early age. *Constr Build Mater* 2015; 75: 11–18.
- Chen IA, Hargis CW and Juenger MCG. Understanding expansion in calcium sulfoaluminate-belite cements. *Cem Concr Res* 2012; 42: 51–60.
- Pace ML, Telesca A, Marroccoli M, et al. Use of industrial byproducts as alumina sources for the synthesis of calcium sulfoaluminate cements. *Environ Sci Technol* 2011; 45: 6124–6128.
- Telesca A, Marroccoli M, Tomasulo M, et al. Calcium looping spent sorbent as a limestone replacement in the manufacture of portland and calcium sulfoaluminate cements. *Environ Sci Technol* 2015; 49: 6865–6871.
- Telesca A, Marroccoli M, Tomasulo M, et al. Low-CO<sub>2</sub> cements from fluidized bed process wastes and other industrial by-products. *Combust Sci Technol* 2016; 188: 492–503.
- Sirtoli D, Tortelli S, Riva P, et al. Mechanical and environmental performances of sulpho-based rapid hardening concrete. In: *SP-305: Durability and Sustainability of Concrete Structures*. Farmington Hills, MI: American Concrete Institute, 2015, SP-305–47.
- Coppola L, Coffetti D and Crotti E. Use of tartaric acid for the production of sustainable Portland-free CSA-based mortars. *Construction and Building Materials* 2018; 171: 243–249.
- Glasser F and Zhang L. High-performance cement matrices based on calcium sulfoaluminate–belite compositions. *Cem Concr Res* 2001; 31: 1881–1886.
- Janotka I, Krajčič L, Ray A, et al. The hydration phase and pore structure formation in the blends of sulfoaluminate-belite cement with Portland cement. *Cem Concr Res* 2003; 33: 489–497.

16. Aranda MAG and De la Torre AG. Sulfoaluminate cement. In: Pacheco-Torgal F, Jalali S, Labrincha J, et al. (eds) *Eco-efficient concrete*. Amsterdam: Elsevier, 2013, pp. 488–522.
17. Trauchessec R, Mechling JM, Lecomte A, et al. Hydration of ordinary Portland cement and calcium sulfoaluminate cement blends. *Cem Concr Compos* 2015; 56: 106–114.
18. Gastaldi D, Canonico F and Boccaleri E. Ettringite and calcium sulfoaluminate cement: investigation of water content by near-infrared spectroscopy. *J Mater Sci* 2009; 44: 5788–5794.
19. Winnefeld F and Lothenbach B. Hydration of calcium sulfoaluminate cements—Experimental findings and thermodynamic modelling. *Cem Concr Res* 2010; 40: 1239–1247.
20. Telesca A, Marroccoli M, Tomasulo M, et al. Hydration properties and technical behavior of calcium sulfoaluminate cements. In: *ACI Special Publication*. Farmington Hills, MI: American Concrete Institute, 2015, pp. 237–254.
21. Telesca A, Marroccoli M, Pace ML, et al. A hydration study of various calcium sulfoaluminate cements. *Cem Concr Compos* 2014; 53: 224–232.
22. Canonico F, Bernardo G, Buzzi L, et al. Microstructural investigations on hydrated high-performance cements based on calcium sulfoaluminate. In: *12th International Congress on the Chemistry of Cement*. Montreal, Canada, 2007, p. W3 11.4.
23. Kasselouri V, Tsakiridis P, Malami C, et al. A study on the hydration products of a non-expansive sulfoaluminate cement. *Cem Concr Res* 1995; 25: 1726–1736.
24. Juenger MCG, Winnefeld F, Provis JL, et al. Advances in alternative cementitious binders. *Cem Concr Res* 2011; 41: 1232–1243.
25. Pelletier L, Winnefeld F and Lothenbach B. The ternary system Portland cement-calcium sulfoaluminate clinker-anhydrite: Hydration mechanism and mortar properties. *Cem Concr Compos* 2010; 32: 497–507.
26. Hargis CW, Kirchheim AP, Monteiro PJM, et al. Early age hydration of calcium sulfoaluminate (synthetic ye'elimite, C<sub>4</sub>A<sub>3</sub>S̄) in the presence of gypsum and varying amounts of calcium hydroxide. *Cem Concr Res* 2013; 48: 105–115.
27. Hargis CW, Lothenbach B, Müller CJ, et al. Carbonation of calcium sulfoaluminate mortars. *Cem Concr Compos* 2017; 80: 123–134.
28. Bernardo G, Telesca A and Valenti GL. A porosimetric study of calcium sulfoaluminate cement pastes cured at early ages. *Cem Concr Res* 2006; 36: 1042–1047.
29. Valenti GL, Marroccoli M, Pace ML, et al. Discussion of the paper understanding expansion in calcium sulfoaluminate-belite cements by I.A. Chen et al., *Cem. Concr. Res.* 42 (2012) 51–60. *Cem Concr Res* 2012; 42: 1555–1559.
30. Beretka J, Marroccoli M, Sherman N, et al. The influence of C<sub>4</sub>A<sub>3</sub>S̄ content and W/S ratio on the performance of calcium sulfoaluminate-based cements. *Cem Concr Res* 1996; 26: 1673–1681.
31. Guo X, Shi H, Hu W, et al. Durability and microstructure of CSA cement-based materials from MSWI fly ash. *Cem Concr Compos* 2013; 46: 26–31.
32. Zhang L and Glasser FP. Investigation of the microstructure and carbonation of CSA-based concretes removed from service. *Cem Concr Res* 2005; 35: 2252–2260.
33. Ioannou S, Paine K and Quillin K. Performance of calcium sulfoaluminate-based concretes. Paper presented at *International Conference on Non-Conventional Materials and Technologies: Ecological Materials and Technologies for Sustainable Building*, Cairo, Egypt.
34. Duan P, Chen W, Ma J, et al. Influence of layered double hydroxides on microstructure and carbonation resistance of sulfoaluminate cement concrete. *Chin Cer Soc* 2013; 42: 1042–1046.
35. Li C, Sun H and Li L. A review: The comparison between alkali-activated slag (Si + Ca) and metakaolin (Si + Al) cements. *Cem Concr Res* 2010; 40: 1341–1349.
36. Pacheco-Torgal, F, Labrincha, JA, Leonelli, C, et al. (eds). *Handbook of alkali-activated cements, mortars and concretes*. Amsterdam: Elsevier, 2015.
37. Bernal SA, Provis JL, Fernandez-Jimenez A, et al. Binder chemistry—High-calcium-activated materials. In: Provis J and van Deventer J (eds) *Alkali activated materials. State-of-the-art report, RILEM TC 224-AAM*. London, UK: Springer, 2014. pp. 59–85.
38. Lamuta C, Candamano S, Crea F, et al. Direct piezoelectric effect in geopolymeric mortars. *Mater Des* 2016; 107: 57–64.
39. Candamano S, Frontera P, Macario A, et al. Preparation and characterization of active Ni-supported catalyst for syngas production. *Chem Eng Res Des* 2015; 96: 78–86.
40. Candamano S, Frontera P, Macario A, et al. New material as Ni-support for hydrogen production by ethanol conversion. *WIT Trans Eng Sci* 2014; 2014: 115–122.
41. Bakharev T, Sanjayan JG and Cheng YB. Effect of admixtures on properties of alkali-activated slag concrete. *Cem Concr Res* 2000; 30: 1367–1374.
42. Shi C, Krivenko PV and Roy DM. *Alkali-activated cements and concretes*. Boca Raton: Taylor & Francis, 2006.
43. García-Lodeiro I, Fernández-Jiménez A and Palomo A. Variation in hybrid cements over time. Alkaline activation of fly ash-portland cement blends. *Cem Concr Res* 2013; 52: 112–122.
44. Garcia-Lodeiro I, Fernández Jimémez AM and Palomo A. Hydration kinetics in hybrid binders: Early reaction stages. *Cem Concr Compos* 2013; 39: 82–92.
45. García-Lodeiro I, Fernández-Jiménez A, Palomo A, et al. Effect of calcium additions on N-A-S-H cementitious gels. *J Am Ceram Soc* 2010; 93: 1934–1940.
46. Balon I, Nikulin Y, Muravev V, et al. Slag formation in production of steelmaking pig-iron. *Steel USSR* 1973; 4: 268–273.
47. Fernández-Jiménez A and Puertas F. Alkali-activated slag cements: Kinetic studies. *Cem Concr Res* 1997; 27: 359–368.
48. Bernal SA, Provis JL, Rose V, et al. Evolution of binder structure in sodium silicate-activated slag-metakaolin blends. *Cem Concr Compos* 2011; 33: 46–54.
49. Myers RJ, Bernal SA, San Nicolas R, et al. Generalized structural description of calcium-sodium aluminosilicate

- hydrate gels: The cross-linked substituted tobermorite model. *Langmuir* 2013; 29: 5294–5306.
50. Puertas F. Escorias de alto horno: composición y comportamiento hidráulico. *Mater Construcción* 1993; 43: 37–48.
  51. Fernández Jiménez AM. Cementos de escorias activadas alcalinamente influencia de las variables y modelización del proceso. PhD Thesis, Autonomous University of Madrid, Spain, 2000.
  52. Rajaokarivony-Andriambololona Z, Thomassin JH, Baillif P, et al. Experimental hydration of two synthetic glassy blast furnace slags in water and alkaline solutions (NaOH and KOH 0.1 N) at 40°C: structure, composition and origin of the hydrated layer. *J Mater Sci* 1990; 25: 2399–2410.
  53. Roy A, Schilling PJ, Eaton HC, et al. Activation of ground blast-furnace slag by alkali-metal and alkaline-earth hydroxides. *J Am Ceram Soc* 1992; 75: 3233–3240.
  54. Duxson P, Provis JL, Lukey GC, et al. Understanding the relationship between geopolymer composition, microstructure and mechanical properties. *Colloids Surf A Physicochem Eng Asp* 2005; 269: 47–58.
  55. Puertas F, Palacios M, Manzano H, et al. A model for the C-A-S-H gel formed in alkali-activated slag cements. *J Eur Ceram Soc* 2011; 31: 2043–2056.
  56. Lothenbach B and Gruskovnjak A. Hydration of alkali-activated slag: thermodynamic modelling. *Adv Cem Res* 2007; 19: 81–92.
  57. Fernandez-Jimenez A and Puertas F. Effect of activator mix on the hydration and strength behaviour of alkali-activated slag cements. *Adv Cem Res* 2003; 15: 129–136.
  58. Ben Haha M, Lothenbach B, Le Saout G, et al. Influence of slag chemistry on the hydration of alkali-activated blast-furnace slag - Part II: Effect of Al<sub>2</sub>O<sub>3</sub>. *Cem Concr Res* 2012; 42: 74–83.
  59. Zhang YJ, Zhao YL, Li HH, et al. Structure characterization of hydration products generated by alkaline activation of granulated blast furnace slag. *J Mater Sci* 2008; 43: 7141–7147.
  60. Bigozzi MC, Manzi S, Lancellotti I, et al. Mix-design and characterization of alkali activated materials based on metakaolin and ladle slag. *Appl Clay Sci* 2013; 73: 78–85.
  61. Provis JL and Bernal SA. Geopolymers and related alkali-activated materials. *Annu Rev Mater Res* 2014; 44: 299–327.
  62. Singh B, Ishwarya G, Gupta M, et al. Geopolymer concrete: A review of some recent developments. *Constr Build Mater* 2015; 85: 78–90.
  63. Provis JL, Palomo A and Shi C. Advances in understanding alkali-activated materials. *Cem Concr Res* 2015; 78: 110–125.
  64. Zhuang XY, Chen L, Komarneni S, et al. Fly ash-based geopolymer: Clean production, properties and applications. *J Clean Prod* 2016; 125: 253–267.
  65. Bigozzi MC, Manzi S, Natali ME, et al. Room temperature alkali activation of fly ash: The effect of Na<sub>2</sub>O/SiO<sub>2</sub> ratio. *Constr Build Mater* 2014; 69: 262–270.
  66. Natali Murri A, Rickard WDA, Bigozzi MC, et al. High temperature behaviour of ambient cured alkali-activated materials based on ladle slag. *Cem Concr Res* 2013; 43: 51–61.
  67. Carabba L, Manzi S, Rambaldi E, et al. High-temperature behaviour of alkali-activated composites based on fly ash and recycled refractory particles. *J Ceram Sci Technol* 2017; 8: 377–388.
  68. Colangelo F, Cioffi R, Roviello G, et al. Thermal cycling stability of fly ash based geopolymer mortars. *Compos Part B Eng* 2017; 129: 11–17.
  69. Zhang Z, Yao X, Zhu H, et al. Activating process of geopolymer source material: Kaolinite. *J Wuhan Univ Technol Mater Sci Ed* 2009; 24: 132–136.
  70. Ambroise J, Murat M and Pera J. Investigations on synthetic binders obtained by middle-temperature thermal dissociation of clay minerals. *Silic Ind* 1986; 7: 99–107.
  71. Singh PS, Trigg M, Bugar I, et al. Geopolymer formation processes at room temperature studied by <sup>29</sup>Si and <sup>27</sup>Al MAS-NMR. *Mater Sci Eng A* 2005; 396: 392–402.
  72. Zuhua Z, Xiao Y, Huajun Z, et al. Role of water in the synthesis of calcined kaolin-based geopolymer. *Appl Clay Sci* 2009; 43: 218–223.
  73. Rovnanik P. Effect of curing temperature on the development of hard structure of metakaolin-based geopolymer. *Constr Build Mater* 2010; 24: 1176–1183.
  74. Pacheco-Torgal F, Moura D, Ding Y, et al. Composition, strength and workability of alkali-activated metakaolin based mortars. *Constr Build Mater* 2011; 25: 3732–3745.
  75. Mobili A, Belli A, Giosuè C, et al. Metakaolin and fly ash alkali-activated mortars compared with cementitious mortars at the same strength class. *Cem Concr Res* 2016; 88: 198–210.
  76. Provis JL and van Deventer JSJ. *Geopolymers: Structures, Processing, Properties and Industrial Applications*. Cambridge, UK: Woodhead Publishing Limited, 2009.
  77. Zhang Z, Wang H, Yao X, et al. Effects of halloysite in kaolin on the formation and properties of geopolymers. *Cem Concr Compos*. 2012; 34: 709–715.
  78. Zibouche F, Kerdjoudj H, d'Espinose de Lacaillerie JB, et al. Geopolymers from Algerian metakaolin. Influence of secondary minerals. *Appl Clay Sci* 2009; 43: 453–458.
  79. MacKenzie KJD, Brown IWM, Meinhold RH, et al. Outstanding problems in the kaolinite-mullite reaction sequence investigated by <sup>29</sup>Si and <sup>27</sup>Al solid-state nuclear magnetic resonance: I, Metakaolinite. *J Am Ceram Soc* 1985; 68: 293–301.
  80. Rahier H, Denayer JF and Van Mele B. Low-temperature synthesized aluminosilicate glasses: Part IV. Modulated DSC study on the effect of particle size of metakaolinite on the production of inorganic polymer glasses. *J Mater Sci* 2003; 38: 3131–3136.
  81. Zhang Z, Wang H, Provis JL, et al. Quantitative kinetic and structural analysis of geopolymers. Part 1. the activation of metakaolin with sodium hydroxide. *Thermochim Acta* 2012; 539: 23–33.
  82. Duxson P, Mallicoat SW, Lukey GC, et al. The effect of alkali and Si/Al ratio on the development of mechanical properties of metakaolin-based geopolymers. *Colloids Surfaces A Physicochem Eng Asp* 2007; 292: 8–20.
  83. Thomas RJ and Peethamparan S. Alkali-activated concrete: Engineering properties and stress-strain behavior. *Constr Build Mater* 2015; 93: 49–56.

84. Xu H and Van Deventer JSJ. The geopolymerisation of aluminosilicate minerals. *Int J Miner Process* 2000; 59: 247–266.
85. Davidovits J. *Mineral polymers and methods of making them*. Patent 4,349,386, USA, 1982.
86. Yun-Ming L, Cheng-Yong H, Al Bakri MM, et al. Structure and properties of clay-based geopolymer cements: A review. *Prog Mater Sci* 2016; 83: 595–629.
87. He P, Wang M, Fu S, et al. Effects of Si/Al ratio on the structure and properties of metakaolin based geopolymer. *Cer Int* 2016; 14416–14422.
88. Kamaloo A, Ganjkanlou Y, Aboutalebi SH, et al. Modeling of compressive strength of metakaolin based geopolymers by the use of artificial neural network. *Int J Eng A Basics* 2010; 23: 145–152.
89. Lizcano M, Kim HS, Basu S, et al. Mechanical properties of sodium and potassium activated metakaolin-based geopolymers. *J Mater Sci* 2012; 47: 2607–2616.
90. Kuenzel C, Vandeperre LJ, Donatello S, et al. Ambient temperature drying shrinkage and cracking in metakaolin-based geopolymers. *J Am Ceram Soc* 2012; 95: 3270–3207.
91. Kong DLY, Sanjayan JG and Sagoe-Crentsil K. Comparative performance of geopolymers made with metakaolin and fly ash after exposure to elevated temperatures. *Cem Concr Res* 2007; 37: 1583–1589.
92. Perera DS, Uchida O, Vance ER, et al. Influence of curing schedule on the integrity of geopolymers. *J Mater Sci* 2007; 42: 3099–3106.
93. He J, Zhang G, Hou S, et al. Geopolymer-based smart adhesives for infrastructure health monitoring: Concept and feasibility. *J Mater Civ Eng* 2011; 23: 100–109.
94. Yang T, Zhu H and Zhang Z. Influence of fly ash on the pore structure and shrinkage characteristics of metakaolin-based geopolymer pastes and mortars. *Constr Build Mater* 2017; 153: 284–293.
95. Ozga I, Ghedini N, Giosuè C, et al. Assessment of air pollutant sources in the deposit on monuments by multivariate analysis. *Sci Total Environ* 2014; 490: 776–784.
96. Corinaldesi V, Moriconi G and Tittarelli F. Thaumassite: Evidence for incorrect intervention in masonry restoration. *Cem Concr Compos* 2003; 25: 1157–1160.
97. Ozga I, Bonazza A, Bernardi E, et al. Diagnosis of surface damage induced by air pollution on 20th-century concrete buildings. *Atmos Environ* 2011; 45: 4986–4995.
98. Tittarelli F, Moriconi G and Bonazza A. Atmospheric deterioration of cement plaster in a building exposed to a urban environment. *J Cult Herit* 2008; 9: 203–206.
99. Palomo A, Blanco-Varela MT, Granizo ML, et al. Chemical stability of cementitious materials based on metakaolin. *Cem Concr Res* 1999; 29: 997–1004.
100. Gao XX, Michaud P, Joussein E, et al. Behavior of metakaolin-based potassium geopolymers in acidic solutions. *J Non Cryst Solids* 2013; 380: 95–102.
101. Borges PHR, Bantia N, Alcamand HA, et al. Performance of blended metakaolin/blastfurnace slag alkali-activated mortars. *Cem Concr Compos* 2016; 71: 42–52.
102. Okada K, Ooyama A, Isobe T, et al. Water retention properties of porous geopolymers for use in cooling applications. *J Eur Ceram Soc* 2009; 29: 1917–1923.
103. Tittarelli F, Carsana M and Ruello ML. Effect of hydrophobic admixture and recycled aggregate on physical-mechanical properties and durability aspects of no-fines concrete. *Constr Build Mater* 2014; 66: 30–37.
104. Tittarelli F. Effect of low dosages of waste GRP dust on fresh and hardened properties of mortars: Part 2. *Constr Build Mater* 2013; 47: 1539–1543.
105. Tittarelli F, Giosuè C, Mobili A, et al. Effect of using recycled instead of virgin EPS in lightweight mortars. *Procedia Eng* 2016; 161: 660–665.
106. Arellano Aguilar R, Burciaga Diaz O and Escalante Garcia JI. Lightweight concretes of activated metakaolin-fly ash binders, with blast furnace slag aggregates. *Constr Build Mater* 2010; 24: 1166–1175.
107. Duan P, Song L, Yan C, et al. Novel thermal insulating and lightweight composites from metakaolin geopolymer and polystyrene particles. *Ceram Int* 2017; 43: 5115–5120.
108. Medri V, Papa E, Mazzocchi M, et al. Production and characterization of lightweight vermiculite/geopolymer-based panels. *Mater Des* 2015; 85: 266–274.
109. El-Naggar MR and El-Dessouky MI. Re-use of waste glass in improving properties of metakaolin-based geopolymers: Mechanical and microstructure examinations. *Constr Build Mater* 2017; 132: 543–555.
110. Barnat-Hunek D, Siddique R and Łagód G. Properties of hydrophobised lightweight mortars with expanded cork. *Constr Build Mater* 2017; 155: 15–25.
111. Giosuè C, Pierpaoli M, Mobili A, et al. Influence of binders and lightweight aggregates on the properties of cementitious mortars: From traditional requirements to indoor air quality improvement. *Materials* 2017; 10: 978.
112. Tittarelli F, Giosuè C, Mobili A, et al. Influence of binders and aggregates on VOCs adsorption and moisture buffering activity of mortars for indoor applications. *Cem Concr Compos* 2015; 57.
113. Giosuè C, Mobili A, Toscano G, et al. Effect of biomass waste materials as unconventional aggregates in multifunctional mortars for indoor application. *Procedia Eng* 2016; 161: 655–659.
114. Gasca-Tirado JR, Manzano-Ramírez A, Vazquez-Landaverde PA, et al. Ion-exchanged geopolymer for photocatalytic degradation of a volatile organic compound. *Mater Lett* 2014; 134: 222–224.
115. Strini A, Roviello G, Ricciotti L, et al. TiO<sub>2</sub>-based photocatalytic geopolymers for nitric oxide degradation. *Materials* 2016; 9: 513.
116. Bell JL and Kriven WM. Preparation of ceramic foams from metakaolin-based geopolymer gels. *Ceram Eng Sci Proc* 2009; 29: 97–112.
117. Kamseu E, Nait-Ali B, Bignozzi MC, et al. Bulk composition and microstructure dependence of effective thermal conductivity of porous inorganic polymer cements. *J Eur Ceram Soc* 2012; 32: 1593–1603.
118. Zhang HY, Kodur V, Cao L, et al. Fiber reinforced geopolymers for fire resistance applications. *Procedia Eng* 2014; 71: 153–158.
119. Zhang Z, Provis JL, Reid A, et al. Geopolymer foam concrete: An emerging material for sustainable construction. *Construct Build Mater* 2014; 56: 113–127.

120. Kamseu E, Ceron B, Tobias H, et al. Insulating behavior of metakaolin-based geopolymer materials assessed with heat flux meter and laser flash techniques. *J Therm Anal Calorim* 2012; 108: 1189–1199.
121. Duxson P, Lukey GC and van Deventer JSJ. Thermal conductivity of metakaolin geopolymers used as a first approximation for determining gel interconnectivity. *Ind Eng Chem Res* 2006; 45: 7781–7788.
122. Prud'homme E, Michaud P, Joussein E, et al. Silica fume as porogen agent in geo-materials at low temperature. *J Eur Ceram Soc* 2010; 30: 1641–1648.
123. Delair S, Prud'homme É, Peyratout C, et al. Durability of inorganic foam in solution: The role of alkali elements in the geopolymer network. *Corros Sci* 2012; 59: 213–221.
124. Abdul Rahim RH, Rahmiati T, Azizli KA, et al. Comparison of using NaOH and KOH activated fly ash-based geopolymer on the mechanical properties. *Mater Sci Forum* 2015; 803: 179–184.
125. Duxson P, Lukey GC, Separovic F, et al. Effect of alkali cations on aluminum incorporation in geopolymeric gels. 2005; 44: 832–839.
126. Duxson P, Provis GC, Lukey A, et al. <sup>39</sup>K NMR of free potassium in geopolymers. 2006; 45: 9208–9210.
127. Koloušek D, Brus J, Urbanova M, et al. Preparation, structure and hydrothermal stability of alternative (sodium silicate-free) geopolymers. *J Mater Sci* 2007; 42: 9267–9275.
128. Peng MX, Wang ZH, Shen SH, et al. Synthesis, characterization and mechanisms of one-part geopolymeric cement by calcining low-quality kaolin with alkali. *Mater Struct* 2014; 48: 699–708.
129. Feng D, Provis JL and Deventer JSJ. Thermal activation of albite for the synthesis of one-part mix geopolymers. *J Am Ceram Soc* 2012; 95: 565–572.
130. Peys A, Rahier H and Pontikes Y. Potassium-rich biomass ashes as activators in metakaolin-based inorganic polymers. *Appl Clay Sci* 2016; 119: 401–409.
131. Marroccoli M, Pace ML, Telesca A, et al. Utilization of coal combustion ashes for the synthesis of ordinary and special cements. *Combust Sci Technol* 2010; 182: 588–599.
132. Natali ME, White CE and Bignozzi MC. Elucidating the atomic structures of different sources of fly ash using X-ray and neutron PDF analysis. *Fuel* 2016; 177: 148–156.
133. Erdoğan ST and Koçak TÇ. Influence of slag fineness on the strength and heat evolution of multiple-clinker blended cements. *Constr Build Mater* 2017; 155: 800–810.
134. Gong K and White CE. Impact of chemical variability of ground granulated blast-furnace slag on the phase formation in alkali-activated slag pastes. *Cem Concr Res* 2016; 89: 310–319.
135. Bernal SA, Mejía de Gutiérrez R, et al. Effect of binder content on the performance of alkali-activated slag concretes. *Cem Concr Res* 2011; 41: 1–8.
136. Kamseu E, Rizzuti A, Leonelli C, et al. Enhanced thermal stability in K<sub>2</sub>O-metakaolin-based geopolymer concretes by Al<sub>2</sub>O<sub>3</sub> and SiO<sub>2</sub> fillers addition. *J Mater Sci* 2010; 45: 1715–1724.
137. Carabba L, Santandrea M, Carloni C, et al. Steel fiber reinforced geopolymer matrix (S-FRGM) composites applied to reinforced concrete structures for strengthening applications: A preliminary study. *Compos Part B Eng* 2017; 128: 83–90.
138. Monticelli C, Natali ME, Balbo A, et al. A study on the corrosion of reinforcing bars in alkali-activated fly ash mortars under wet and dry exposures to chloride solutions. *Cem Concr Res* 2016; 87: 53–63.
139. Nematollahi B and Sanjayan J. Effect of different superplasticizers and activator combinations on workability and strength of fly ash based geopolymer. *Mater Des* 2014; 57: 667–672.
140. Carabba L, Manzi S and Bignozzi MC. Superplasticizer addition to carbon fly ash geopolymers activated at room temperature. *Materials* 2016; 9: 9070586.
141. Law DW, Adam AA, Molyneux TK, et al. Long term durability properties of class F fly ash geopolymer concrete. *Mater Struct* 2015; 48: 721–731.
142. Coppola L, Lorenzi S, Kara P, et al. Performance and compatibility of phosphonate-based superplasticizers for concrete. *Buildings* 2017; 7: 62.
143. Coppola L, Lorenzi S, Garlati S, et al. The rheological and mechanical performances of concrete manufactured with blended admixtures based on phosphonates. *Key Eng Mater* 2016; 674: 159–164.
144. Coppola L, Buoso A and Lorenzi S. Compatibility issues of NSF-PCE superplasticizers with several lots of different cement types (long-term results). *Kuei Suan Jen Hsueh Pao/J Chin Ceram Soc* 2010; 38(9).
145. Monticelli C, Natali ME, Balbo A, et al. Corrosion behavior of steel in alkali-activated fly ash mortars in the light of their microstructural, mechanical and chemical characterization. *Cem Concr Res* 2016; 80: 60–68.
146. Coppola L, Coffetti D and Crotti E. Innovative carboxylic acid waterproofing admixture for self-sealing watertight concretes. *Construction and Building Materials* 2018; 171: 817–824.
147. He C, Osbaeck B and Makovicky E. Pozzolanic reactions of six principal clay minerals: Activation, reactivity assessments and technological effects. *Cem Concr Res* 1995; 25: 1691–1702.
148. Chen JH, Huang JS and Chang YW. A preliminary study of reservoir sludge as a raw material of inorganic polymers. *Constr Build Mater* 2009; 23: 3264–3269.
149. De Vincenzo A, Jacopo Molino A, Molino B, et al. Reservoir rehabilitation: The new methodological approach of Economic Environmental Defence. *Int J Sediment Res* 2017; 32: 288–294.
150. Chiang KY, Chien KL and Hwang SJ. Study on the characteristics of building bricks produced from reservoir sediment. *J Hazard Mater* 2008; 159: 499–504.
151. Tang CW, Chen HJ, Wang SY, et al. Production of synthetic lightweight aggregate using reservoir sediments for concrete and masonry. *Cem Concr Compos* 2011; 33: 292–300.
152. Liao YC and Huang CY. Effects of CaO addition on lightweight aggregates produced from water reservoir sediment. *Constr Build Mater* 2011; 25: 2997–3002.
153. Liao Y-C and Huang C-Y. Effects of heat treatment on the physical properties of lightweight aggregate from water reservoir sediment. *Ceram Int* 2011; 37: 3723–3730.

154. Ferone C, Colangelo F, Cioffi R, et al. Use of reservoir clay sediments as raw materials for geopolymer binders. *Adv Appl Ceram* 2013; 112: 184–189.
155. Ferone C, Liguori B, Capasso I, et al. Thermally treated clay sediments as geopolymer source material. *Appl Clay Sci* 2015; 107: 195–204.
156. Molino B, De Vincenzo A, Ferone C, et al. Recycling of clay sediments for geopolymer binder production. A new perspective for reservoir management in the framework of Italian Legislation: The Occhito reservoir case study. *Materials* 2014; 7: 5603–5616.
157. Messina F, Ferone C, Molino A, et al. Synergistic recycling of calcined clayey sediments and water potabilization sludge as geopolymer precursors: Upscaling from binders to precast paving cement-free bricks. *Constr Build Mater* 2017; 133: 14–26.
158. Peirce S, Santoro L, Andini S, et al. Clay sediment geopolymerization by means of alkali metal aluminate activation. *RSC Adv* 2015; 5: 107662–107669.
159. Goosens A. Verwertung von Wasserwerksschlamm und deren Probleme. *GWF-Wass Abwass* 1996; 137: 17–20.
160. Huang C, Pan JR and Liu Y. Mixing water treatment residual with excavation waste soil in brick and artificial aggregate making. *J Environ Eng* 2005; 131: 272–277.
161. Coppola L, Lorenzi S and Pellegrini S. Rheological and mechanical performances of concrete manufactured by using washing water of concrete mixing transport trucks. In: *ACI Special Publication*. Farmington Hills, MI: American Concrete Institute, 2015. pp. 187–200.
162. Ramadan M, Fouad H and Hassanain A. Reuse of water treatment plant sludge in brick manufacturing. *J Appl Sci Res* 2008; 4: 1223–1229.
163. Monosi S, Troli R, Coppola L, et al. Water reducers for the high alumina cement-silica fume system. *Materials and Structures/Materiaux et Constructions* 1996; 29(194): 639–644.
164. Husillos Rodríguez N, Martínez-Ramírez S, Blanco-Varela MT, et al. Evaluation of spray-dried sludge from drinking water treatment plants as a prime material for clinker manufacture. *Cem Concr Compos* 2011; 33: 267–275.
165. Huang CH and Wang SY. Application of water treatment sludge in the manufacturing of lightweight aggregate. *Constr Build Mater* 2013; 43: 174–183.
166. Coppola L, Troli R, Collepardi S, et al. Innovative cementitious materials from HPC to RPC - Part II. The effect of cement and silica fume type on the compressive strength of reactive powder concrete [Materiali cementizi innovativi: Dagli HPC verso gli RPC - Parte II. L'influenza del cemento e del fumo di silice sulla resistenza meccanica del reactive powder concrete]. *Industria del cemento* 1996; 66(707): 112–125.
167. Lirer S, Liguori B, Capasso I, et al. Mechanical and chemical properties of composite materials made of dredged sediments in a fly-ash based geopolymer. *J Environ Manage* 2017; 191: 1–7.
168. Cabrini M, Lorenzi S, Pastore T, et al. EIS and voltammetry study of passive film formation on steel bar embedded in Portland cement and innovative cementitious binder. In: *10th International Symposium on Electrochemical Impedance Spectroscopy [Book of Abstracts]*. Toxa, Galicia, Spain, 19–24 June 2016. University of Bergamo: Aisberg.
169. Coppola L, Lorenzi S and Pastore T. Qualificazione dei nuovi leganti per il confezionamento di calcestruzzi in relazione alla protezione delle armature. *AIMAT, Nuovi orizzonti della ricerca LEGANTI, CALCETSRUZZI E MATERIALI INNOVATIVI PER COSTRUIRE SOSTENIBILE*, in *Onore di Giuseppe Frigione*, Cosenza, 2015.
170. Cabrini M, Coppola L, Lorenzi S, et al. Valutazione del comportamento a corrosione i calcestruzzi confezionati con leganti innovativi. In: *XI Giornate Nazionali sulla Corrosione e Protezione*. Ferrara, Italy, 15–17 June 2015. University of Bergamo: Aisberg.
171. Glasser FP and Zhang L. High-performance cement matrices based on calcium sulfoaluminate-belite compositions. *Cem Concr Res* 2001; 31: 1881–1886.
172. Kalogridis D, Kostoglouidis GC, Ftikos C, et al. Quantitative study of the influence of non-expansive sulfoaluminate cement on the corrosion of steel reinforcement. *Cem Concr Res* 2000; 30: 1731–1740.
173. Gastaldi D, Canonico F, Capelli L, et al. In situ tomographic investigation on the early hydration behaviors of cementing systems. *Constr Build Mater* 2012; 29: 284–290.
174. Zhang D, Xu D, Cheng X, et al. Carbonation resistance of sulphoaluminate cement-based high performance concrete. *J Wuhan Univ Technol Mater Sci Ed* 2009; 24: 663–666.
175. Andac M and Glasser FP. Pore solution composition of calcium sulfoaluminate cement. *Adv Cem Res* 1999; 11: 23–26.
176. Carsana M, Bianchi M, Canonico F, et al. Corrosion behaviour of steel embedded in calcium sulphoaluminate-cement concrete. In: *14th International Congress on the Chemistry of Cement (ICCC 2015)*, Beijing, China, 13–16 October, 2015.
177. Zhao J, Cai G, Gao D, et al. Influences of freeze-thaw cycle and curing time on chloride ion penetration resistance of Sulphoaluminate cement concrete. *Constr Build Mater* 2014; 53: 305–311.
178. Jen G, Stompinis N and Jones R. Chloride ingress in a belite-calcium sulfoaluminate cement matrix. *Cem Concr Res* 2017; 98: 130–135.
179. Janotka I and Krajči L. An experimental study on the upgrade of sulfoaluminate—belite cement systems by blending with Portland cement. *Adv Cem Res* 1999; 11: 35–41.
180. Pouhet R and Cyr M. Carbonation in the pore solution of metakaolin-based geopolymer. *Cem Concr Res* 2016; 88: 227–235.
181. Babae M and Castel A. Chloride-induced corrosion of reinforcement in low-calcium fly ash-based geopolymer concrete. *Cem Concr Res* 2016; 88: 96–107.
182. Angst U, Elsener B, Larsen C, et al. Critical chloride content in reinforced concrete — A review. *Cem Concr Res* 2009; 39: 1122–12238.
183. Page CL. Mechanism of corrosion protection in reinforced concrete marine structures. *Nature* 1975; 258: 514–515.
184. Cabrini M, Lorenzi S and Pastore T. Cyclic voltammetry evaluation of inhibitors for localised corrosion in alkaline solutions. *Electrochim Acta* 2014; 124: 156–164.

185. Cabrini M, Lorenzi S and Pastore T. Studio della corrosione localizzata degli acciai per armature in soluzioni alcaline inibite - 39BRG. *La Metall Ital* 2013; 105: 21–31.
186. Hausmann DA. Steel corrosion in concrete—How does it occur? *Mater Prot* 1967; 6:19–23.
187. Gouda VK. Corrosion and corrosion inhibition of reinforcing steel: I. Immersed in alkaline solutions. *Br Corros J* 1970; 5: 198–203.
188. Goni S and Andrade C. Synthetic concrete pore solution chemistry and rebar corrosion rate in the presence of chlorides. *Cem Concr Res* 1990; 20: 525–539.
189. Wedding P and Diamond S. Chloride concentrations in concrete pore solutions resulting from calcium and sodium chloride admixtures. *Cem Concr Aggregates* 1986; 8: 97–102.
190. Yonezawa T, Ashworth V and Procter RPM. Pore solution composition and chloride effects on the corrosion of steel in concrete. *Corrosion* 1988; 44: 489–499.
191. Alonso MC and Sanchez M. Analysis of the variability of chloride threshold values in the literature. *Mater Corros* 2009; 60: 631–637.
192. Bolzoni F, Coppola L, Goidanich S, et al. Corrosion inhibitors in reinforced concrete structures Part 1: Preventative technique. *Corros Eng Sci Technol* 2004; 39: 219–228.
193. Pastore T, Cabrini M, Coppola L, et al. Evaluation of the corrosion inhibition of salts of organic acids in alkaline solutions and chloride contaminated concrete. *Mater Corros* 2011; 62: 187–195.
194. De Weerd K, Colombo A, Coppola L, et al. Impact of the associated cation on chloride binding of Portland cement paste. *Cem Concr Res* 2015; 68: 196–202.
195. Glass G and Buenfeld N. The presentation of the chloride threshold level for corrosion of steel in concrete. *Corros Sci* 1997; 39: 1001–1013.
196. Carsana M, Tittarelli F and Bertolini L. Use of no-fines concrete as a building material: Strength, durability properties and corrosion protection of embedded steel. *Cem Concr Res* 2013; 48: 64–73.
197. Tittarelli F, Carsana M and Bellezze T. Corrosion behavior of reinforced no-fines concrete. *Corros Sci* 2013; 70: 119–126.
198. Mobili A, Belli A, Giosuè C, et al. Corrosion behaviour of bare and galvanized steel in geopolymeric and cementitious mortars with the same strength class exposed to chlorides. *Corros Sci* 2016; 134: 64–77.
199. Mobili A, Belli A, Giosuè C, et al. Comportamento a corrosione di armature zincate in malte geopolimeriche e cementizie a parità di classe di resistenza. [Corrosion behavior of galvanized steel reinforcements in geopolymeric and cementitious mortars at the same strength class]. *Metall Ital* 2017; 7: 47–50.
200. Mobili A, Giosuè C, Belli A, et al. *Geopolymeric and cementitious mortars with the same mechanical strength class: Performances and corrosion behaviour of black and galvanized steel bars*. In: American Concrete Institute, International Concrete Abstracts Portal 305: 18-1–18-10, 2015.
201. Aguirre-Guerrero AM, Robayo-Salazar RA and de Gutiérrez RM. A novel geopolymer application: Coatings to protect reinforced concrete against corrosion. *Appl Clay Sci* 2017; 135: 437–446.
202. Bernal SA, Provis JL, Brice DG, et al. Accelerated carbonation testing of alkali-activated binders significantly underestimates service life: The role of pore solution chemistry. *Cem Concr Res* 2012; 42: 1317–1326.
203. Cyr M and Pouhet R. Carbonation in the pore solution of metakaolin-based geopolymer. *Cem Concr Res* 2016; 88: 227–335.
204. Cabrini M, Lorenzi S and Pastore T. Studio elettrochimico della formazione del film di passività sulle armature nel calcestruzzo. In: *Giornate Nazionali della Corrosione*. Naples Italy, 10–12 July 2013.
205. Cabrini M, Lorenzi S and Pastore T. Steel damaging in flowing mortar. *Corros Eng Sci Technol* 2016; 51: 596–605.
206. Bertolini L, Elsener B, Redaelli E, et al. *Corrosion of steel in concrete: Prevention, diagnosis, repair*. 2nd ed. Weinheim: Wiley, 2013.
207. Bertolini L, Bolzoni F, Pastore T, et al. Behaviour of stainless steel in simulated concrete pore solution. *Br Corros J* 1996; 31: 218–222.
208. Bertolini L and Gastaldi M. Corrosion resistance of low-nickel duplex stainless steel rebars. *Mater Corros* 2011; 62: 120–129.
209. Gastaldi M and Bertolini L. Effect of temperature on the corrosion behaviour of low-nickel duplex stainless steel bars in concrete. *Cem Concr Res* 2014; 56: 52–60.
210. Bertolini L, Gastaldi M, Pedferri P, et al. Factors influencing the corrosion resistance of austenitic and duplex stainless steel bars in chloride bearing concrete. In: *Proceedings of 15th International Corrosion Congress 2002: Frontiers in Corrosion Science and Technology*. Granada, Spain, 22–27 September, 2002.
211. Coppola L, Cadoni E, Forni D, et al. Mechanical characterization of cement composites reinforced with fiberglass, carbon nanotubes or glass reinforced plastic (GRP) at high strain rates. *Appl Mech Mater* 2011; 82: 190–195.
212. Criado M, Bastidas DM, Fajardo S, et al. Corrosion behaviour of a new low-nickel stainless steel embedded in activated fly ash mortars. *Cem Concr Compos* 2011; 33: 644–652.
213. Monticelli C, Criado M, Fajardo S, et al. Corrosion behaviour of a Low Ni austenitic stainless steel in carbonated chloride-polluted alkali-activated fly ash mortar. *Cem Concr Res* 2014; 55: 49–58.
214. Morgan DR. Compatibility of concrete repair materials and systems. *Constr Build Mater* 1996; 10: 57–67.
215. Schueremans L, Cizer Ö, Janssens E, et al. Characterization of repair mortars for the assessment of their compatibility in restoration projects: Research and practice. *Constr Build Mater* 2011; 25: 4338–4350.
216. Van Balen K, Papayianni I, Van Hees, et al. Introduction to requirements for and functions and properties of repair mortars. *Mater Struct* 2005; 38: 781–785.
217. Bertolini L, Coppola L, Gastaldi M, et al. Electroosmotic transport in porous construction materials and dehumidification of masonry. *Constr Build Mater* 2009; 23: 254–263.
218. Coppola L. Repair and conservation of reinforced concrete tent-church by Pino Pizzigoni at Longuelo-Bergamo



- (Italy). *International Journal of Architectural Heritage* 2018; 1–9.
219. Fournier B and Bérubé M-A. Alkali-aggregate reaction in concrete: a review of basic concepts and engineering implications. *Can J Civ Eng* 2000; 27: 167–191.
  220. Collepardi M. Thaumassite formation and deterioration in historic buildings. *Cem Concr Compos* 1999; 21: 147–154.
  221. Veiga MR, Velosa AL and Magalhães AC. Evaluation of mechanical compatibility of renders to apply on old walls based on a restrained shrinkage test. *Mater Struct* 2007; 40: 1115–1126.
  222. Lanas J and Alvarez JI. Masonry repair lime-based mortars: Factors affecting the mechanical behavior. *Cem Concr Res* 2003; 33: 1867–1876.
  223. Veiga MR, Aguiar J, Santos Silva A, et al. Methodologies for characterisation and repair of mortars of ancient buildings. *Hist Constr Int Semin* 2001; January: 353–362.
  224. Maravelaki-Kalaitzaki P, Bakolas A, Karatasios I, et al. Hydraulic lime mortars for the restoration of historic masonry in Crete. *Cem Concr Res* 2005; 35: 1577–1586.
  225. Lanas J, Bernal JLP, Bello MA, et al. Mechanical properties of natural hydraulic lime-based mortars. *Cem Concr Res* 2004; 34: 2191–2201.
  226. Lanas J, Sirera R and Alvarez JI. Study of the mechanical behavior of masonry repair lime-based mortars cured and exposed under different conditions. *Cem Concr Res* 2006; 36: 961–970.
  227. Roy DM. Alkali-activated cements: Opportunities and challenges. *Cem Concr Res* 1999; 29: 249–254.
  228. Coppola L, Lorenzi S and Buoso A. Electric arc furnace granulated slag as a partial replacement of natural aggregates for concrete production. In: *2nd International Conference on Sustainable Construction Materials and Technologies*. Ancona, Italy, 28–30 June 2010.
  229. Coppola L, Buoso A, Coffetti D, et al. Electric arc furnace granulated slag for sustainable concrete. *Constr Build Mater* 2016; 123: 115–119.
  230. Coppola L, Lorenzi S, Marcassoli P, et al. Concrete production by using cast iron industry by-products [Impiego di sottoprodotti dell'industria siderurgica nel confezionamento di calcestruzzo per opere in c.a. e c.a.p. *Industria Italiana del Cemento* 2007; 77.
  231. Wang SD, Scrivener KL and Pratt PL. Factors affecting the strength of alkali-activated slag. *Cem Concr Res* 1994; 24: 1033–1043.
  232. Wang S-D, Pu X-C, Scrivener KL, et al. Alkali-activated slag cement and concrete: a review of properties and problems. *Adv Cem Res* 1995; 7: 93–102.
  233. Pal SC, Mukherjee A and Pathak SR. Investigation of hydraulic activity of ground granulated blast furnace slag in concrete. *Cem Concr Res* 2003; 33: 1481–1486.
  234. Escalante-García JI, Fuentes AF, Gorokhovskiy A, et al. Hydration products and reactivity of blast-furnace slag activated by various alkalis. *J Am Ceram Soc* 2003; 86: 2148–2153.
  235. Brough AR and Atkinson A. Sodium silicate-based, alkali-activated slag mortars - Part I. Strength, hydration and microstructure. *Cem Concr Res* 2002; 32: 865–879.
  236. Collins FG and Sanjayan JG. Workability and mechanical properties of alkali activated slag concrete. *Cem Concr Res* 1999; 29: 455–458.
  237. Bernal S, San Nicolas R, Provis J, et al. Alkali-activated slag cements produced with a blended sodium carbonate / sodium silicate activator. *Adv Cem Res* 2015; 28: 1–12.
  238. Coppola L, Coffetti D and Crotti E. Pre-packed alkali activated cement-free mortars for repair of existing masonry buildings and concrete structures. *Construction and building materials* 2018; 173: 111–117.
  239. Provis JL. Alkali-activated materials. *Cem Concr Res*. Epub ahead of print 2 March 2017. DOI: 10.1016/j.cemconres.2017.02.009.
  240. Wongpa J, Kiattikomol K, Jaturapitakkul C, et al. Compressive strength, modulus of elasticity, and water permeability of inorganic polymer concrete. *Mater Des* 2010; 31: 4748–4754.
  241. Oh JE, Clark SM and Monteiro PJM. Does the Al substitution in C–S–H(I) change its mechanical property? *Cem Concr Res* 2011; 41: 102–106.
  242. Lee NK, Jang JG and Lee HK. Shrinkage characteristics of alkali-activated fly ash/slag paste and mortar at early ages. *Cem Concr Compos* 2014; 53: 239–248.
  243. Collins F and Sanjayan J. Effect of pore size distribution on drying shrinking of alkali-activated slag concrete. *Cem Concr Res* 2000; 30: 1401–1406.
  244. Li Z, Zhao X, He T, et al. A study of high-performance slag-based composite admixtures. *Constr Build Mater* 2017; 155: 126–136.
  245. Alderete N, Villagrán Y, Mignon A, et al. Pore structure description of mortars containing ground granulated blast-furnace slag by mercury intrusion porosimetry and dynamic vapour sorption. *Constr Build Mater* 2017; 145: 157–165.
  246. Ye H, Cartwright C, Rajabipour F, et al. Understanding the drying shrinkage performance of alkali-activated slag mortars. *Cem Concr Compos* 2017; 76: 13–24.
  247. Ye H and Radlińska A. Shrinkage mechanisms of alkali-activated slag. *Cem Concr Res* 2016; 88: 126–135.
  248. Palacios M and Puertas F. Effect of shrinkage-reducing admixtures on the properties of alkali-activated slag mortars and pastes. *Cem Concr Res* 2007; 37: 691–702.
  249. Bilim C, Karahan O, Atiş CD and Ilkentapar S. Influence of admixtures on the properties of alkali-activated slag mortars subjected to different curing conditions. *Mater Des* 2013; 44: 540–547.
  250. Najafi Kani E, Allahverdi A and Provis JL. Efflorescence control in geopolymer binders based on natural pozzolan. *J Therm Anal Calorim* 2012; 34: 25–33.
  251. Allahverdi A, Najafi Kani E and Shaverdi B. Carbonation versus efflorescence in alkali-activated blast-furnace slag in relation with chemical composition of activator. *Int J Civ Eng* 2017; 15: 565–573.